Published in final edited form as:
Curr Biol. 2009 July 14; 19(13): 1133–1139. doi:10.1016/j.cub.2009.05.022.

The Rho-linked Mental Retardation Protein OPHN1 Controls Synaptic Vesicle Endocytosis Via Endophilin A1

Akiko Nakano-Kobayashi[1], **Nael Nadif Kasri**[1], **Sarah E. Newey**[1], and **Linda Van Aelst**[1,*]
[1]Cold Spring Harbor Laboratory, 1 Bungtown Road, Cold Spring Harbor, New York, 11724, USA

Abstract

Summary—Neurons transmit information at chemical synapses by releasing neurotransmitters that are stored in synaptic vesicles (SVs) at the presynaptic site. After release, these vesicles need to be efficiently retrieved in order to maintain synaptic transmission [1–3]. In concurrence, malfunctions in SV recycling have been associated with cognitive disorders [4,5]. *Oligophrenin-1 (OPHN1)* encodes a Rho-GTPase activating protein (Rho-GAP) whose loss-of-function causes X-linked mental retardation [6,7]. OPHN1 is highly expressed in the brain and present both pre- and post-synaptically in neurons [8]. Previous studies report that postsynaptic OPHN1 is important for dendritic spine morphogenesis [8,9], but its function at the presynaptic site remains largely unexplored. Here, we present evidence that reduced/defective OPHN1 signaling impairs SV cycling at hippocampal synapses. In particular, we show that OPHN1 knockdown affects the kinetic efficiency of endocytosis. We further demonstrate that OPHN1 forms a complex with endophilin A1, a protein implicated in membrane curvature generation during SV endocytosis [10–16], and, importantly, that OPHN1's interaction with endophilin A1 and its Rho-GAP activity are important for its function in SV endocytosis. Our findings suggest that defects in efficient SV retrieval may contribute to the pathogenesis of *OPHN1*-linked cognitive impairment.

Results and Discussion

OPHN1 Is Important for Efficient SV Endocytosis

We demonstrated previously that OPHN1 is present at presynaptic sites of hippocampal neurons, and is concentrated in axonal boutons that stain positive for synaptophysin [8, and Figure S1]. Presynaptic boutons are sophisticated compartments designed for the regulated release of neurotransmitters via SVs. Since a synaptic terminal in the brain typically contains only 100–200 SVs, they must be recycled to maintain efficient neurotransmitter release during ongoing activity [1–3]. Multiple mechanisms have been reported for SV retrieval; among them clathrin-mediated endocytosis is believed to be a major physiological mechanism at hippocampal synapses [3,17–23].

To explore a potential role for OPHN1 in SV cycling, we examined SV uptake at presynaptic terminals of hippocampal neurons in which OPHN1 expression was reduced by RNA interference (RNAi). As shown in Figure S2, RNAi using short hairpin RNAs (shRNAs) targeting the coding sequence (Ophn1#1) or the 3' untranslated region (3'UTR; Ophn1#2) of

*Correspondence: E-mail: vanaelst@cshl.edu; Phone: 516-367-6829; Fax: 516-367-8815.

rat OPHN1 mRNA, but not a scrambled control shRNA (scr#1), dramatically reduced OPHN1 levels in hippocampal neurons. The fluorescent styryl dye FM4-64, which becomes trapped in SVs upon endocytosis, was then used to assess the effect of OPHN1 knockdown on SV uptake [24]. Briefly, hippocampal neurons were co-transfected with a synaptophysin-EGFP expression vector (to label presynaptic boutons) and vectors expressing Ophn1#1, Ophn1#2, scr#1, or no shRNA. FM4-64 dye was loaded into SVs by depolarizing neurons with KCl. After collecting FM4-64 staining images, the neurons were subjected to a second KCl stimulus to unload the dye (Figure 1A). Interestingly, neurons expressing Ophn1#1 or Ophn1#2 shRNA displayed a significantly reduced uptake of FM4-64 dye in their presynaptic boutons when compared to empty control vector or scr#1 shRNA expressing neurons (Figures 1A–1B). Similar results were obtained when Ophn1 shRNAs were introduced into hippocampal neurons by lentiviral transduction (Figure 1C and Figure S2). To ensure that the reduction in FM4-64 uptake was specifically caused by impaired OPHN1 expression, we performed rescue experiments using OPHN1 cDNA that lacks the 3'UTR and is therefore resistant to Ophn1#2 shRNA mediated RNAi. The levels of OPHN1 expression in neurons co-expressing RNAi-resistant OPHN1-WT and Ophn1#2 shRNA were restored to normal levels (Figure S2), and, most importantly, the extent of FM4-64 accumulation in presynaptic boutons was comparable to that of control neurons (Figures 1A–1C). These data indicate that the observed effect of OPHN1 RNAi is specific.

The reduction in FM4-64 dye uptake in OPHN1 RNAi expressing neurons could be due to aberrations in a number of processes, including impairment in SV endocytosis, reduction in number of SVs available for release, and/or a defect in SV release kinetics. A first hint for a potential role of OPHN1 in controlling the rate of SV endocytosis came from our experiments where the time of FM4-64 dye exposure following stimulation was varied (30 s versus 3 min) and the more physiological electrical field stimulation was used to load and unload the dye (Figures 1D–1E). Specifically, in one set of experiments, neurons were stimulated at 10 Hz for 30 s in the presence of dye, and the dye was immediately washed out (Figure 1D), whereas in the other set the dye was left for an additional 2.5 min after the 30-s stimulation (Figure 1E). In both cases, the total dye uptake was assessed in subsequent maximal unloading rounds of stimulation. Without delay of the wash, the total amount of internalized dye was reduced by ~50% in Ophn1#2 shRNA expressing neurons compared to scr#1 shRNA expressing neurons (Figure 1D). In contrast, only a reduction of ~15 % was observed when the dye was left for a total of 3 min (Figure 1E), suggesting that over time OPHN1 depleted neurons could take up similar amounts of dye as the control neurons, but doing so at a slower rate.

To further investigate this, we measured the kinetics of SV endocytosis following electrical stimulation [24,25]. Specifically, Ophn1#2 and scr#1 shRNA expressing neurons were presented with FM4-64 dye for 3 min after a variable delay time Δt following the start of a 300 action potential (AP) stimulus train, and the total dye uptake was quantified in subsequent unloading rounds of stimulation (Figure 1F). Notably, as the interval of Δ*t* is increased, more endocytosis occurs before the dye exposure, and, hence, less dye is incorporated into the vesicle pool. We observed a significant reduction in the kinetics of dye uptake in neurons expressing Ophn1#2 shRNA compared to scr#1 shRNA expressing neurons, with 50% of maximal uptake ($t_{1/2}$) occurring within ~53 s for Ophn1#2 shRNA and ~27 s for scr#1 shRNA (Figure 1F). This reduction was rescued by co-expressing RNAi-resistant OPHN1-WT with Ophn1#2 shRNA ($t_{1/2}$ of ~28 s, Figure 1F). These data imply that knockdown of OPHN1 in synaptic terminals slows down SV endocytosis. Importantly, when examining the kinetics of FM4-64 dye unloading in neurons expressing Ophn1#2 or scr#1 shRNA, we found that the kinetics of dye unloading was not significantly different between neurons expressing Ophn1#2 shRNA and those expressing scr#1 shRNA (Figure S3), indicating that the slowed endocytosis is not due to an alteration in the rate of SV exocytosis. Thus, our data support a role for OPHN1 in

controlling the kinetic efficiency of endocytosis. The additional involvement of OPHN1 in other step(s) of the SV recycling process is however not excluded.

Presynaptic OPHN1 Knockdown Impairs Efficacy of Synaptic Transmission Under High Frequency Stimulation

Next, we performed electrophysiological experiments to gain insight into the functional consequences of impaired presynaptic OPHN1 expression. For these experiments, the presynaptic CA3 area of hippocampal brain slices was infected with a high-titer lentivirus expressing either scr#1 or Ophn1#2 shRNA, together with EGFP. A stimulating electrode was then positioned in the heavily infected cell body area in CA3 to activate CA3 axons expressing Ophn1#2 or scr#1 shRNA. Recordings of evoked responses (EPSCs) were made from uninfected pyramidal neurons in the CA1 region (Figure 2A).

We investigated the impact of presynaptic OPHN1 knockdown on glutamatergic synaptic transmission under high-frequency stimulation conditions that produce short-term synaptic depression. Under these conditions, the number of SVs available for release becomes rate-limited due to a variety of factors, including the replenishment of the readily releasable pool of SVs (RRP) by vesicle retrieval [22,27]. In this regard, increased synaptic depression has been observed when key SV endocytosis components were perturbed [13,14,27,28]. Interestingly, we found that upon repetitive stimulation at 10 Hz (100 stimuli), the EPSC amplitude in CA1 neurons receiving their input from Ophn1#2 shRNA expressing CA3 neurons decreased more rapidly and reached a significantly lower plateau compared to the EPSC amplitude in CA1 neurons receiving their input from scr#1 shRNA expressing CA3 neurons (Figures 2B–2C). Furthermore, when examining the effect of multiple train stimulations on the EPSC amplitude, we also found that CA1 neurons receiving their input from Ophn1#2 shRNA expressing CA3 neurons exhibited a significantly steeper decrease in the EPSC amplitude compared to that in neurons receiving their input from scr#1 shRNA expressing CA3 neurons (Figure 2D). Importantly, the steeper decrease in EPSC amplitudes was rescued by co-expressing RNAi-resistant OPHN1-WT with Ophn1#2 shRNA in the CA3 neurons (Figures 2B–D). The difference in EPSC amplitudes after train stimulations strongly suggests that replenishment of the RRP is hindered in Ophn1#2 shRNA expressing CA3 neurons. In view of our finding that OPHN1 affects endocytosis kinetics, we infer that this impediment likely reflects impaired SV endocytosis caused by OPHN1 knockdown; although a contribution from other mechanisms cannot be excluded. It is worth mentioning that we did not observe any defect in paired-pulse facilitation in OPHN1 knockdown neurons at all interstimulus intervals assayed (Figure 2E), implying that the integrity of the presynaptic release machinery was not appreciably affected by OPHN1 knockdown. Overall, our findings indicate that presynaptic OPHN1 is important for maintaining synaptic efficacy during repetitive firing at hippocampal synapses.

Identification of Endophilin A1 as an OPHN1 Interacting Protein

To gain insight into how OPHN1 affects SV retrieval, we searched for OPHN1 interacting proteins by performing a yeast two-hybrid (YTH) screen. Interestingly, two of the positive clones contained identical cDNAs matching the entire sequence of endophilin A1. Endophilin A1 is a member of the endophilin family that is primarily expressed in the brain, and has been implicated in several stages of SV endocytosis [10,13–16]. It contains an N-terminal N-BAR (Bin/Amphiphysin/Rvs-homology) domain that drives membrane curvature, and a C-terminal SH3 domain [11,12].

The interaction between OPHN1 and endophilin A1 was rigorously tested by several different approaches. First, the YTH interaction (Figure S4) was confirmed by GST-fusion protein pull-down assays (Figure 3A). Second, to demonstrate an *in vivo* association between OPHN1 and

endophilin A1, co-immunoprecipitation experiments were carried out using lysates prepared from mouse brain. An anti-OPHN1 antibody co-immunoprecipitated endophilin A1 from brain lysates, and vice versa an anti-endophilin 1 antibody co-immunoprecipitated OPHN1 (Figure 3B). Finally, we performed co-localization studies in hippocampal neurons and found that endogenously expressed OPHN1 and endophilin A1 proteins colocalize in axonal boutons (Figure S4). Together, these results indicate that OPHN1 and endophilin A1 form a complex *in vivo*.

We next set out to identify the endophilin A1 binding region in OPHN1. The OPHN1 protein contains several interesting protein motifs: a BAR and Pleckstrin-homology (PH) domain at its N-terminus, and a GAP domain shown to negatively regulate Rho proteins [8], followed by three successive proline rich domains (PRDs) at its C-terminus (Figure 3C). We generated a series of OPHN1 deletion mutants and tested them for their ability to interact with full-length endophilin A1 using the YTH system (Figures 3C–3D). Only OPHN1 fragments that contain the PRDs were able to interact with endophilin A1 (Figure 3D). Given that PRDs serve as docking sites for SH3 domains and endophilin A1 contains an SH3 domain, we reasoned that OPHN1 is likely to bind to endophilin A1 via one of its PRDs. To examine this, amino acid substitutions were introduced into the first (PRD1*), second (PRD2*) or third (PRD3*) PRD of full-length OPHN1 (Figure 3C). Wild type and mutant OPHN1-EGFP fusion proteins were then tested for their ability to bind endophilin A1 in GST-fusion pull down assays (Figure 3E). In contrast to OPHN1-PRD1* and OPHN1-PRD2* mutants, the OPHN1-PRD3* mutant failed to interact with endophilin A1. Also, an OPHN1 deletion mutant lacking the entire PRD3 domain (OPHN1ΔPRD3) failed to bind endophilin A1 (Figures 3C and 3E), indicating that the third PRD is critical for OPHN1's interaction with endophilin A1.

To directly demonstrate that the SH3 domain of endophilin A1 is sufficient for binding to OPHN1, we performed pull-down assays using the isolated SH3 domain fused to GST and lysates from HEK293T cells expressing OPHN1-EGFP. Figure 3F shows that this domain indeed is sufficient to bind to OPHN1. Endophilin A1 has previously been shown to interact with other proteins, including dynamin-1, a GTPase whose activity is required for vesicle fission [29]. This prompted us to look at interactions between endophilin A1, OPHN1, and dynamin-1. We found that endophilin A1 can bind to both OPHN1 and dynamin-1, and OPHN1 to both endophilin A1 and dynamin-1 -suggesting a potential interaction network (Figure S5).

OPHN1's Interaction with Endophilin A1 and Its Rho-GAP Activity Are Required for its Role in SV Endocytosis

To determine whether OPHN1's interaction with endophilin A1 is important for its role in SV retrieval, we tested whether reintroduction of the OPHN1-PRD3* mutant, which is defective in endophilin A1 binding, could rescue the reduction in FM4-64 dye uptake and in endocytosis kinetics observed in Ophn1#2 shRNA expressing neurons. Neurons expressing Ophn1#2 shRNA together with EGFP, RNAi-resistant OPHN1-WT or OPHN1-PRD3* were subjected to FM4-64 dye experiments as described above. In contrast to OPHN1-WT, reintroduction of OPHN1-PRD3* failed to rescue both the reduction in FM4-64 dye uptake and in endocytosis kinetics (Figures 4A–4B). Notably, OPHN1-WT and OPHN1-PRD3* were expressed at similar levels (Figure 4C), and the OPHN1-PRD3* mutant was still concentrated in presynaptic boutons (Figure S6). These data indicate that the interaction of OPHN1 with endophilin A1 is important for OPHN1's function in the SV retrieval process. The mechanistic details of the OPHN1/endophilin A1 interaction remain to be established. Our imaging data suggest that OPHN1 binding to endophilin A1 is not essential for its localization to synaptic boutons and that other domain(s) in OPHN1 and/or interaction(s) likely mediate this. Nevertheless, given the presence of an N-BAR and BAR domain in endophilin A1 and OPHN1, respectively, these proteins when present in a complex could cooperate in the sensing and generation of membrane

curvature at endocytic pits/sites. Indeed, the BAR + PH domain of OPHN1 has been shown to tubulate liposomes [30].

Previous work had linked the GAP activity of OPHN1 to the RhoA/Rho-kinase pathway for spine length regulation [8]. Given that Rho proteins have been implicated in endocytic trafficking, we tested whether the Rho-GAP activity of OPHN1 is also important for its function in SV retrieval. To this end, we generated an OPHN1 mutant, OPHN1-GAP, which virtually lacks Rho-GAP activity (Figure S7). We confirmed that OPHN1-GAP was still able to bind endophilin A1 (Figure S8) and showed a similar subcellular distribution pattern as OPHN1-WT (Figure S6). Co-expression of OPHN1-GAP with Ophn1#2 shRNA failed to rescue the decrease in FM4-64 uptake and reduction in endocytosis kinetics caused by OPHN1 knockdown (Figures 4A–4C). Thus, these data imply that OPHN1's Rho-GAP activity is also important for its role in SV endocytosis.

Conclusions

Previous studies have reported that the X-linked mental retardation protein OPHN1 is important for dendritic spine morphogenesis [8,9]. Here we show that OPHN1 is required for efficient SV retrieval, and that the underlying mechanism involves its interaction with endophilin A1 and Rho GTPases. Increasing evidence points to a link between malfunctions in SV recycling and cognitive deficits [4,5]. For example, decreased SV recycling efficiency and cognitive deficits have been reported in mice deficient in amphiphysin, a clathrin accessory factor [4]. Thus, our findings suggest that besides defects in dendritic spine morphogenesis, inefficient SV endocytosis is likely to contribute to the pathogenesis of *OPHN1*-linked mental retardation.

Supplementary Material

Refer to Web version on PubMed Central for supplementary material.

Acknowledgments

We thank members of the Van Aelst lab, Bo Li, Jacek Skowronski, Darrin Lewis, Martin Wienisch and Dinu Albeanu for discussions and/or critical reading of the manuscript. This work was supported by NAAR and NIH grants to LVA. ANK is a recipient of the Astellas Foundation Fellowship Award (Japan). NNK is a postdoctoral fellow from the Fund for Scientific Research Flanders and is supported by the Human Frontiers Science Program.

References

1. Murthy VN, De Camilli P. Cell biology of the presynaptic terminal. Annu Rev Neurosci 2003;26:701–728. [PubMed: 14527272]
2. Schweizer FE, Ryan TA. The synaptic vesicle: cycle of exocytosis and endocytosis. Curr Opin Neurobiol 2006;16:298–304. [PubMed: 16707259]
3. Tyler WJ, Murthy VN. Synaptic vesicles. Curr Biol 2004;14:R294–R297. [PubMed: 15084295]
4. Di Paolo G, Sankaranarayanan S, Wenk MR, Daniell L, Perucco E, Caldarone BJ, Flavell R, Picciotto MR, Ryan TA, Cremona O, De Camilli P. Decreased synaptic vesicle recycling efficiency and cognitive deficits in amphiphysin 1 knockout mice. Neuron 2002;33:789–804. [PubMed: 11879655]
5. D'Adamo P, Welzl H, Papadimitriou S, Raffaele di Barletta M, Tiveron C, Tatangelo L, Pozzi L, Chapman PF, Knevett SG, Ramsay MF, Valtorta F, Leoni C, Menegon A, Wolfer DP, Lipp HP, Toniolo D. Deletion of the mental retardation gene Gdi1 impairs associative memory and alters social behavior in mice. Hum Mol Genet 2002;11:2567–2580. [PubMed: 12354782]
6. Billuart P, Bienvenu T, Ronce N, des Portes V, Vinet MC, Zemni R, Roest Crollius H, Carrie A, Fauchereau F, Cherry M, Briault S, Hamel B, Fryns JP, Beldjord C, Kahn A, Moraine C, Chelly J. Oligophrenin-1 encodes a rhoGAP protein involved in X-linked mental retardation. Nature 1998;392:923–926. [PubMed: 9582072]

7. Nadif Kasri N, Van Aelst L. Rho-linked genes and neurological disorders. Pflugers Arch 2008;455:787–797. [PubMed: 18004590]
8. Govek EE, Newey SE, Akerman CJ, Cross JR, Van der Veken L, Van Aelst L. The X-linked mental retardation protein oligophrenin-1 is required for dendritic spine morphogenesis. Nat Neurosci 2004;7:364–372. [PubMed: 15034583]
9. Khelfaoui M, Denis C, van Galen E, de Bock F, Schmitt A, Houbron C, Morice E, Giros B, Ramakers G, Fagni L, Chelly J, Nosten-Bertrand M, Billuart P. Loss of X-linked mental retardation gene oligophrenin1 in mice impairs spatial memory and leads to ventricular enlargement and dendritic spine immaturity. J Neurosci 2007;27:9439–9450. [PubMed: 17728457]
10. Ringstad N, Gad H, Low P, Di Paolo G, Brodin L, Shupliakov O, De Camilli P. Endophilin/SH3p4 is required for the transition from early to late stages in clathrin-mediated synaptic vesicle endocytosis. Neuron 1999;24:143–154. [PubMed: 10677033]
11. Masuda M, Takeda S, Sone M, Ohki T, Mori H, Kamioka Y, Mochizuki N. Endophilin BAR domain drives membrane curvature by two newly identified structure-based mechanisms. Embo J 2006;25:2889–2897. [PubMed: 16763557]
12. Gallop JL, Jao CC, Kent HM, Butler PJ, Evans PR, Langen R, McMahon HT. Mechanism of endophilin N-BAR domain-mediated membrane curvature. Embo J 2006;25:2898–2910. [PubMed: 16763559]
13. Verstreken P, Kjaerulff O, Lloyd TE, Atkinson R, Zhou Y, Meinertzhagen IA, Bellen HJ. Endophilin mutations block clathrin-mediated endocytosis but not neurotransmitter release. Cell 2002;109:101–112. [PubMed: 11955450]
14. Schuske KR, Richmond JE, Matthies DS, Davis WS, Runz S, Rube DA, van der Bliek AM, Jorgensen EM. Endophilin is required for synaptic vesicle endocytosis by localizing synaptojanin. Neuron 2003;40:749–762. [PubMed: 14622579]
15. Guichet A, Wucherpfennig T, Dudu V, Etter S, Wilsch-Brauniger M, Hellwig A, Gonzalez-Gaitan M, Huttner WB, Schmidt AA. Essential role of endophilin A in synaptic vesicle budding at the Drosophila neuromuscular junction. Embo J 2002;21:1661–1672. [PubMed: 11927550]
16. Farsad K, Ringstad N, Takei K, Floyd SR, Rose K, De Camilli P. Generation of high curvature membranes mediated by direct endophilin bilayer interactions. J Cell Biol 2001;155:193–200. [PubMed: 11604418]
17. Rizzoli SO, Betz WJ. Synaptic vesicle pools. Nat Rev Neurosci 2005;6:57–69. [PubMed: 15611727]
18. He L, Wu LG. The debate on the kiss-and-run fusion at synapses. Trends Neurosci 2007;30:447–455. [PubMed: 17765328]
19. Dickman DK, Horne JA, Meinertzhagen IA, Schwarz TL. A slowed classical pathway rather than kiss-and-run mediates endocytosis at synapses lacking synaptojanin and endophilin. Cell 2005;123:521–533. [PubMed: 16269341]
20. Heerssen H, Fetter RD, Davis GW. Clathrin dependence of synaptic-vesicle formation at the Drosophila neuromuscular junction. Curr Biol 2008;18:401–409. [PubMed: 18356056]
21. Granseth B, Odermatt B, Royle SJ, Lagnado L. Clathrinmediated endocytosis is the dominant mechanism of vesicle retrieval at hippocampal synapses. Neuron 2006;51:773–786. [PubMed: 16982422]
22. Granseth B, Odermatt B, Royle SJ, Lagnado L. Clathrin-mediated endocytosis: the physiological mechanism of vesicle retrieval at hippocampal synapses. J Physiol 2007;585:681–686. [PubMed: 17599959]
23. Zhu Y, Xu J, Heinemann SF. Two pathways of synaptic vesicle retrieval revealed by single-vesicle imaging. Neuron 2009;61:397–411. [PubMed: 19217377]
24. Cousin MA. Use of FM1-43 and other derivatives to investigate neuronal function. Curr Protoc Neurosci 2008;Chapter 2Unit 2 6
25. Nicholson-Tomishima K, Ryan TA. Kinetic efficiency of endocytosis at mammalian CNS synapses requires synaptotagmin I. Proc Natl Acad Sci U S A 2004;101:16648–16652. [PubMed: 15492212]
26. Newton AJ, Kirchhausen T, Murthy VN. Inhibition of dynamin completely blocks compensatory synaptic vesicle endocytosis. Proc Natl Acad Sci U S A 2006;103:17955–17960. [PubMed: 17093049]

27. Kavalali ET. Multiple vesicle recycling pathways in central synapses and their impact on neurotransmission. J Physiol 2007;585:669–679. [PubMed: 17690145]

28. Chen Y, Deng L, Maeno-Hikichi Y, Lai M, Chang S, Chen G, Zhang JF. Formation of an endophilin-Ca2+ channel complex is critical for clathrin-mediated synaptic vesicle endocytosis. Cell 2003;115:37–48. [PubMed: 14532001]

29. Hinshaw JE. Dynamin and its role in membrane fission. Annu Rev Cell Dev Biol 2000;16:483–519. [PubMed: 11031245]

30. Peter BJ, Kent HM, Mills IG, Vallis Y, Butler PJ, Evans PR, McMahon HT. BAR domains as sensors of membrane curvature: the amphiphysin BAR structure. Science 2004;303:495–499. [PubMed: 14645856]

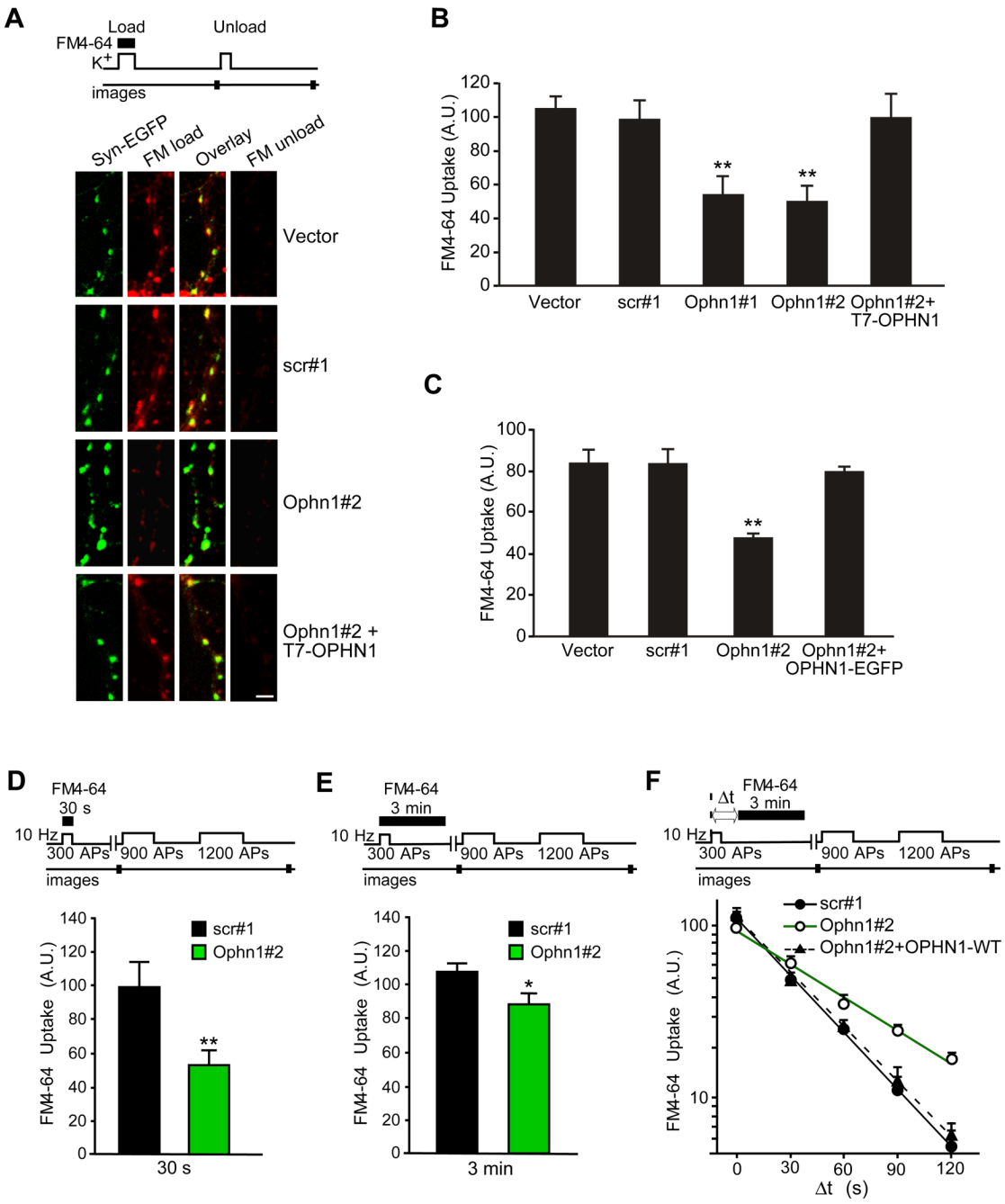

Figure 1. OPHN1 Is Important for Efficient SV Endocytosis

(A–C) Neurons expressing Ophn1 shRNA accumulate significantly less FM4-64.

(A) Top panel, schematic of the FM4-64 labeling experiment. Bottom panel, hippocampal neurons were transfected with indicated plasmids together with a synaptophysin-EGFP expression vector to label presynaptic boutons. Neurons were visualized by fluorescence microscopy after KCl-stimulated loading of FM4-64 dye (red, FM load) and after a 2nd application of KCl to unload the accumulated FM4-64 dye (FM unload); efficient unloading was observed for all conditions. Scale bar, 5 μm.

(B) Quantification of FM4-64 uptake for neurons transfected with the indicated constructs. Data are taken from 4–6 independent experiments (**p< 0.001, t-test, n > 200 boutons per condition). Error bars indicate SEM. A.U. = arbitrary units.
(C) Same as B but for neurons infected with indicated lentiviruses. Data are taken from 4–8 independent experiments (**p< 0.001, t-test, n > 200 boutons per condition).
(D) Top panel, schematic of the FM4-64 labeling experiment. During the loading phase, neurons were stimulated with 300 APs at 10 Hz and exposed to FM4-64 for 30 s. Bottom panel, quantification of FM4-64 uptake for each condition. FM4-64 uptake was assessed by measuring total fluorescence change from images acquired before and after 2 rounds of unloading stimuli (900 and 1200 APs). Data are taken from 5 independent experiments (**p< 0.001, t-test, n > 150 boutons per condition). Error bars indicate SEM.
(E) Same as D, except that neurons were exposed to FM4-64 dye for 3 min. Data are taken from 7 independent experiments (*p< 0.05, t-test, n > 150 boutons per condition).
(F) Slowed endocytosis in OPHN1 depleted synapses. Top panel, schematic of the FM4-64-labeling experiment. During the loading phase, neurons were stimulated with 300 APs at 10 Hz and exposed to FM4-64 for 3 min after a variable delay (Δt) from the onset of the stimulus. Bottom panel, kinetics of endocytosis. Semi-log plot of FM4-64 uptake as a function of Δt in neurons transfected with indicated constructs. Each measurement of Δt was bracketed by runs were Δt=0. Data are taken from 3–7 independent experiments, n >100 boutons per condition. Error bars indicate SEM.
The actual fluorescence intensities represented by A.U. vary between panels B–F, as described in Supplemental Data.

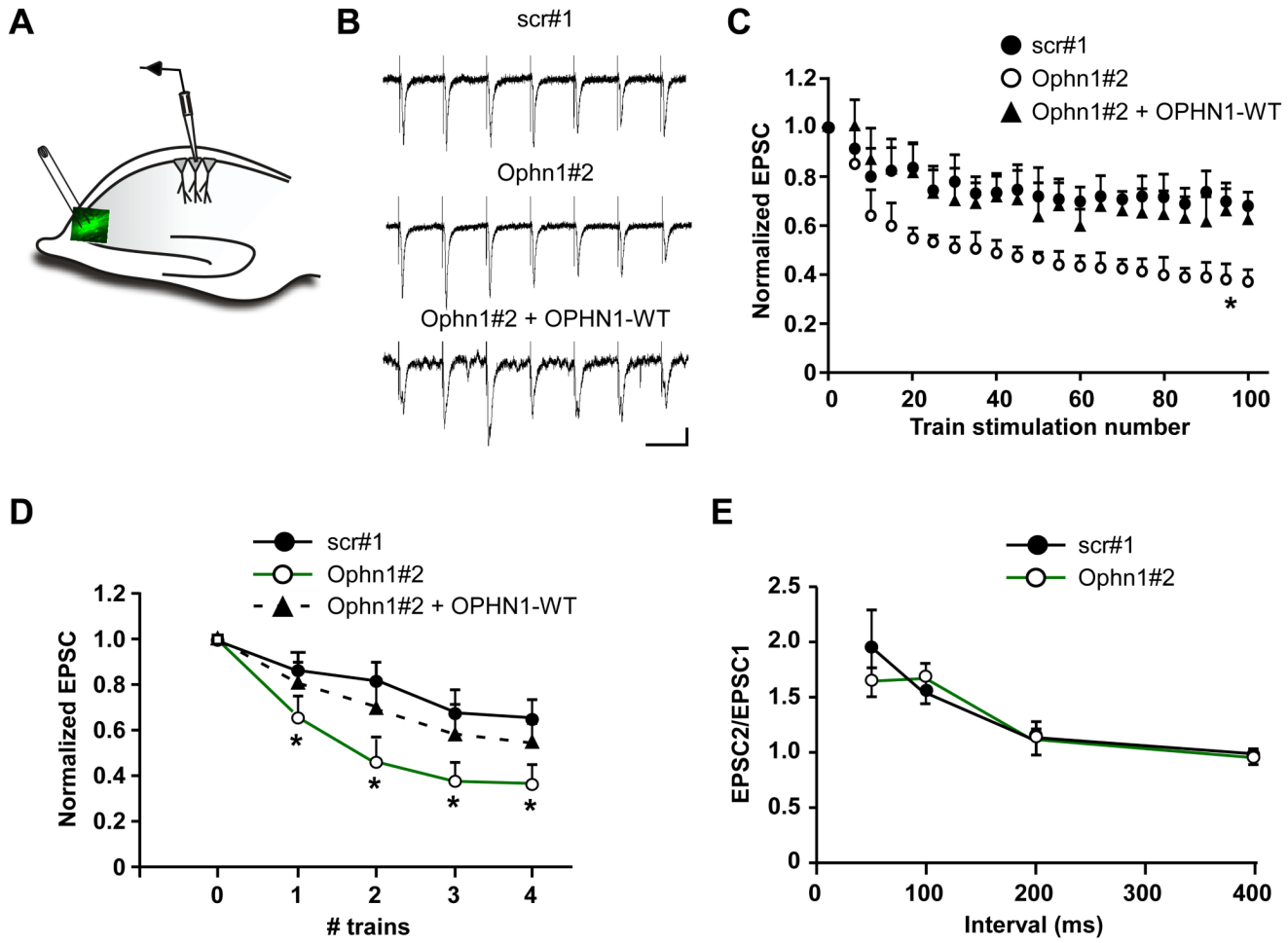

Figure 2. Presynaptic OPHN1 Knockdown Augments Short-Term Synaptic Depression

(A) A diagram of recording configuration at the CA3-CA1 synapse of hippocampal brain slices. EPSC's were recorded from uninfected CA1 neurons that receive their input from CA3 neurons expressing scr#1, Ophn1#2, or Ophn1#2 shRNA and OPHN1-WT-EGFP.

(B) Sample traces (first 7 stimuli from a 100 Hz train) illustrating short-term synaptic depression. Scale: 100 ms, 50 pA.

(C) Normalized EPSC amplitude during the train stimulation (10 Hz, 100 stimuli). *p<0.001, for the last 3 points, t-test, n= 10 cells for all conditions.

(D) Multiple train stimulations (10 Hz, 100 stimuli) were applied with a 1-min interval. EPSC's were recorded at 0.1 Hz in between each train, normalized and averaged to the average EPSC before the first train. *p< 0.05, t-test, n= 10 cells for all conditions.

(E) Paired-pulse ratio (EPSC2/EPSC1) was measured at different interstimulus intervals. p> 0.05, Mann-Whitney test, n= 8 cells for all conditions.

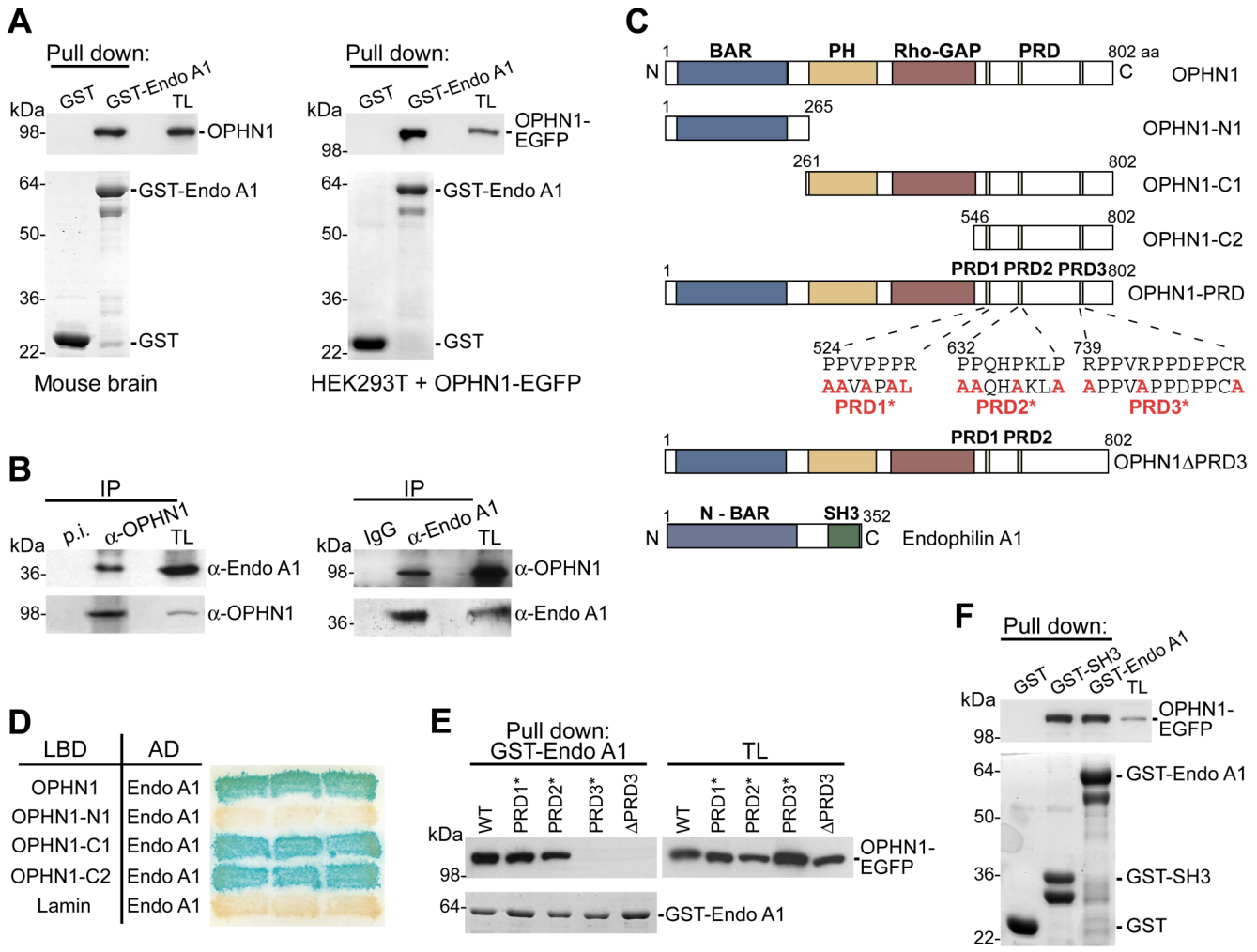

Figure 3. Interaction of OPHN1 with Endophilin A1 (Endo A1)

(A) Endo A1-GST fusion protein, or GST alone, immobilized on glutathione-beads was incubated with extracts from mouse brain (left panel) or with extracts from HEK293T cells expressing OPHN1-EGFP (right panel). Bound OPHN1 was detected by immunoblotting with anti-OPHN1 (left panel) and anti-GFP (right panel) antibody. The GST-fusion proteins used are indicated by Coomassie Brilliant Blue (CBB) staining (lower panels). TL = total lysate.

(B) Mouse brain extract was incubated with pre-immune (p.i.) or anti-OPHN1 serum (left panel), or with rabbit IgG or anti-Endo A1 antibody (right panel). The immuno-precipitates (IP) were analyzed by immunoblotting using indicated antibodies.

(C) Domain structure and deletion and point-mutated constructs of OPHN1 and Endo A1.

(D) YTH interaction between Endo A1 and OPHN1-N- and C-terminal fragments. L40 yeast strain was transformed with plasmids expressing indicated OPHN1 fragments fused to the LexA DNA-binding domain (LBD) and Endo A1 fused to the B42 activation domain (AD), and transformed yeast colonies were assayed for β-galactosidase activity.

(E) Endo A1-GST fusion protein (lower panel, CBB staining) immobilized on beads was incubated with extracts from HEK293T cells expressing OPHN1-WT, OPHN1-PRD1*, -PRD2*, or -PRD3*, or OPHN1ΔPRD3-EGFP fusion proteins. The bound proteins were detected by immunoblotting with anti-GFP antibody.

(F) Endo A1 or Endo A1-SH3 GST fusion protein, or GST alone (lower panel) immobilized on beads was incubated with extracts from HEK293T cells expressing OPHN1-EGFP. Bound OPHN1 was detected by immunoblotting with anti-GFP antibody.

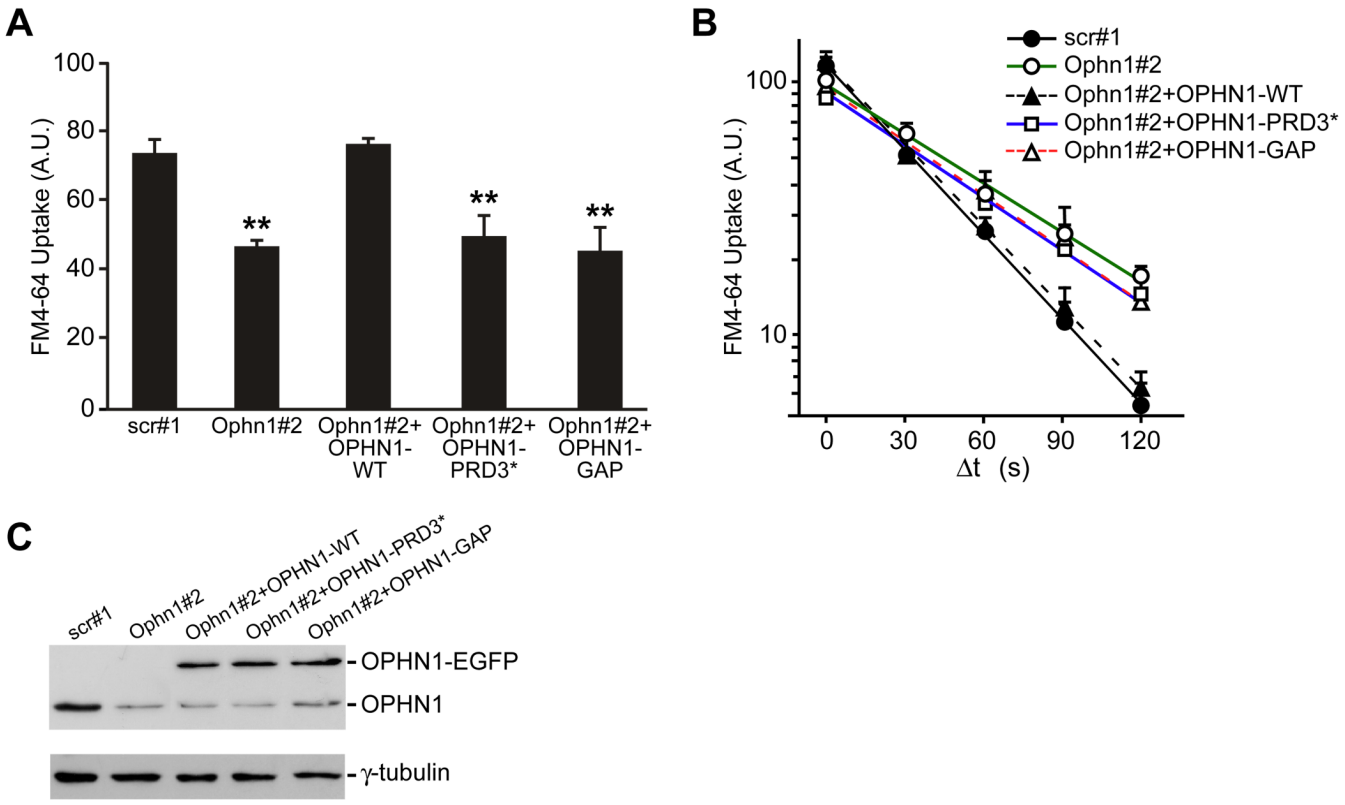

Figure 4. OPHN1/Endophilin A1 Interaction and OPHN1 Rho-GAP Activity Are Important for Efficient SV Endocytosis

(A) Quantification of FM4-64 uptake for neurons transduced with indicated lentiviral vectors. Data are taken from 4–6 independent experiments (**p< 0.001, t-test, n > 200 boutons per condition). Error bars indicate SEM. A.U. = arbitrary units.

(B) Kinetics of endocytosis applying the same protocol as described in Figure 1F. Semi-log plot of FM4-64 uptake as a function of Δt in neurons transfected with indicated constructs. Data are taken from 3–7 independent experiments, n > 100 boutons per condition (scr#1, $t_{1/2}$ of ~27; Ophn1#2, $t_{1/2}$ of ~53; Ophn1#2+OPHN1-WT, $t_{1/2}$ of ~28; Ophn1#2+OPHN1-PRD3*, $t_{1/2}$ of ~50; Ophn1#2+OPHN1-GAP, $t_{1/2}$ of ~45).

(C) Hippocampal neurons were infected at 7 DIV with indicated lentiviral vectors. 8 days post-infection, cell extracts were prepared and analyzed by Western blotting with anti-OPHN1 and anti-γ-tubulin antibody as a loading control.